F-5

Reprinted from

POWDER TECHNOLOGY

Powder Technology 100 (1998) 52–60

Effect of particle shape on the particle size distribution measured with commercial equipment

Makio Naito [a,*], Osamu Hayakawa [a], Kenji Nakahira [a], Hidetoshi Mori [b], JunIchiro Tsubaki [b]

[a] *Research and Development Laboratory, Japan Fine Ceramics Center, 2-4-1 Mutsuno, Atsuta-ku, Nagoya 456-8587, Japan*

[b] *Department of Molecular Design and Engineering, Graduate School of Engineering, Nagoya University, Furo-cho, Chikusa-ku, Nagoya 464-8603, Japan*

Received 14 October 1996; received in revised form 8 January 1997

ELSEVIER

ELSEVIER

Powder Technology 100 (1998) 52–60

POWDER TECHNOLOGY

Effect of particle shape on the particle size distribution measured with commercial equipment

Makio Naito [a,*], Osamu Hayakawa [a], Kenji Nakahira [a], Hidetoshi Mori [b], JunIchiro Tsubaki [b]

[a] *Research and Development Laboratory, Japan Fine Ceramics Center, 2-4-1 Mutsuno, Atsuta-ku, Nagoya 456-8587, Japan*

[b] *Department of Molecular Design and Engineering, Graduate School of Engineering, Nagoya University, Furo-cho, Chikusa-ku, Nagoya 464-8603, Japan*

Received 14 October 1996; received in revised form 8 January 1997

Abstract

The present paper describes the results of a round robin that has been performed to investigate the influence of particle shape on particle-size distributions measured with commercial particle-size analyzers. The commercial equipment based on the five kinds of measuring principle such as electrical sensing zone, laser diffraction and scattering, X-ray sedimentation, photosedimentation, and light-obscuration methods have been employed for analyzing blocky, flaky and rod-like ceramic particles. It is demonstrated that the particle shape has a strong influence on the particle-size distribution measured by the laser diffraction and scattering and by photosedimentation. The size range of rod-like particles is particularly wide when these methods are applied. It is also shown that the particle-size distributions of anisotropic samples measured by photosedimentation has a tendency to be remarkably scattered in the coarse-size range.

Keywords: Particle-size measurement; Round robin; Particle-size analyzer; Particle shape; Fine ceramic powder; Anisotropy shape

1. Introduction

In a new material field such as fine ceramics, not only fine particles having a spherical shape but also flaky-shaped and rod-like particles are often used. The particle shape affects the physical phenomena utilized for particle-size measurement and therefore the results obtained by various measuring principles are influenced by the particle shape [1,2]. The effect of this needs to elucidated. However, the studies on particle shape related to particle-size measurements have not been systematically reported to date.

In our previous round robin on particle-size measurement, the scattering of the measured data with actual commercial analyzers have been systematically analyzed using a fine ceramic raw powder ranging from submicron to micron size. As a result, with respect to particles that are nearly spherical, the degree of scatter among the measured results using various models and measuring principles were clarified [3–5]. However, these results were limited to isotropic particles and the data comparison of measured results with anisotropic particles has not yet been conducted.

With the measured results of anisotropic samples, theoretical investigations using model particles have been reported [6–9]. However, these studies were limited to one measuring principle and not investigated with an actual commercial raw powder. On the other hand, there are a few studies on the comparison of particle size distributions of anisotropic particles measured by various methods [1,2] but only one instrument for each type of method was used. Thus the scatter of data using different models and various measuring principles has not been systematically examined. In practice, many kinds of models are commercialized especially the laser diffraction and scattering and the photosedimentation methods. This means that the scatter of data measured by them should be discussed in detail.

In this paper, a round robin was performed to analyze experimentally the influence of particle shape on the measured results using various commercial particle-size analyzers. Spherical, flaky and rod-like particles generally used in the ceramic industry were selected as samples. On the basis of the results of this round robin, the effect of particle shape on the particle-size distribution and the data scatter of the results from various models and principles has been analyzed.

* Corresponding author.

0032-5910/98/$ - see front matter
PII S0032-5910(98)00052-7

2. Experimental

2.1. Samples

Fig. 1a–d shows the morphology of the samples observed by scanning electron microscopy (SEM) (S-800, Hitachi). The aluminum oxide and barium titanate particles are block-shaped. The boron nitride particles are an irregular flaky shape, the length of the basal plane being between 1 and 10 μm, while the silicon nitride whiskers are rod-like having a length ranging from several microns to 20 μm and a breadth of around 1 μm.

Table 1 shows the physical properties of the samples. The true density was measured by a helium gas pycnometer (Auto Pycnometer 1320, Micromeritics Instrument), the specific surface area was measured by BET gas adsorption method (Quantasorb, Quantachrome), and the refractive index was taken from the literature [10–12].

Table 1
Sample properties

Samples	True density (g/cm^3)	Specific surface area (m^2/g)	Refractive index[a] (−)
Aluminum oxide	3.96	1.9	1.76 [10]
Barium titanate	5.97	1.2	2.40 [10]
Boron nitride	2.29	3.2	1.74 [11]
Silicon nitride whisker	3.15	3.1	2.02 [12]

[a]Literature value.

2.2. Equipment

The particle-size analyzers based on five typical principles were used in the round robin. The details are shown in Table 2 and the number of models used is shown in Table 3.

2.3. Experimental procedures

2.3.1. Sample preparation conditions

In this study, the conditions for sample preparation for the measurements were determined according to the investigation prior to the round robin. Commercial distilled water (Wako) was used as the dispersion medium, and sodium hexametaphosphate and sodium pyrophosphate (Wako, analytical grade) were used as the dispersant agent. The dispersant agent and its concentration were selected by measuring the zeta potential of the sample suspension [3,4,13]. The zeta potential was measured with an electrophoretic analyzer (Lazer Zee Meter Model 501, PEN KEM). Consequently, sodium hexametaphosphate 0.05 wt.% (aq.) for aluminum oxide, sodium hexametaphosphate 0.025 wt.% (aq.) for barium titanate, sodium pyrophosphate 0.025 wt.% (aq.) for boron nitride and sodium hexametaphosphate 0.0125 wt.% (aq.) for the silicon nitride whisker were selected. However, in the measurement of the silicon nitride whisker by photo-sedimentation ethylene glycol was used as the dispersion medium. When water was used as dispersion medium, the

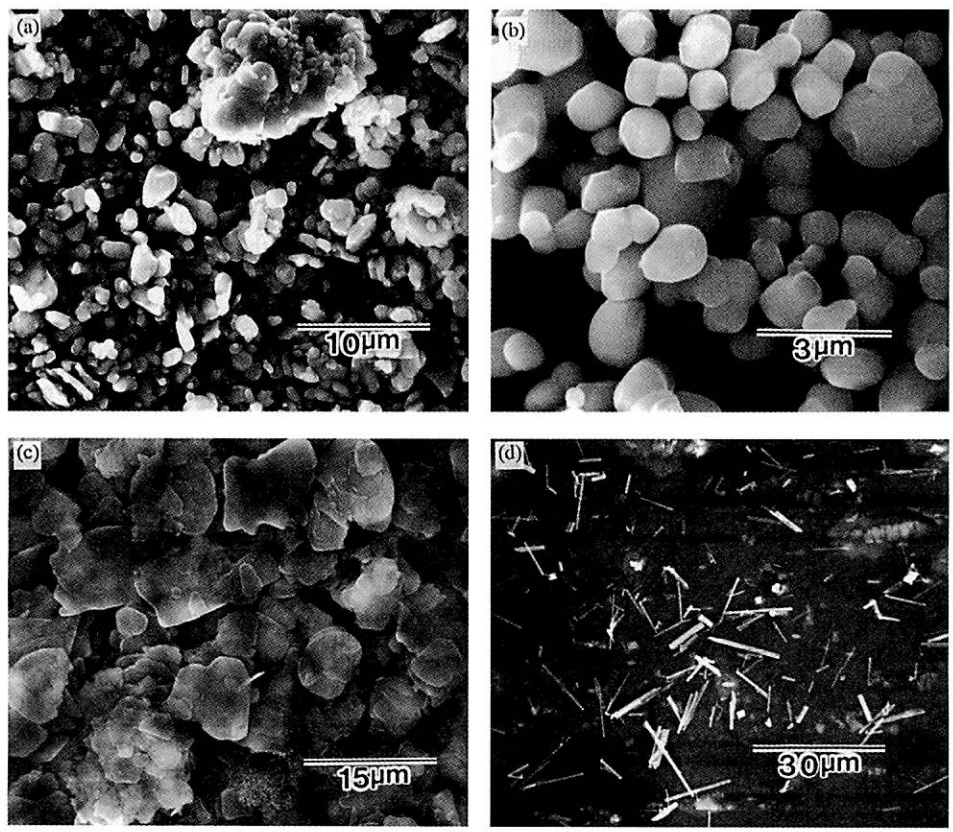

Fig. 1. Scanning electron micrographs: (a) aluminum oxide; (b) barium titanate; (c) boron nitride; (d) silicon nitride whisker.

Table 2
Particle size analyzers used for round robin

Principle	Model	Manufacturer
Laser diffraction and scattering	HELOS	Sympa Tec
	MasterSizer	Malvern
	LA-700, 500	Horiba
	MICROTRAC FRA, SPA	Leeds & Northrup
	HR 850B	Cilas
	SALD-1100, 2000	Shimadzu
	PRO 7000S, LMS-24	Seishin
	LS130	Coulter
Photosedimentation	SKA-5000	Seishin
	CAPA-700	Horiba
	SA-CP4L	Shimadzu
	SA-CP3L	
	SA-CP3	
	SA-CP2	
	BI-DCP 1000	Brookhaven
X-ray sedimentation	SediGraph 5100	Micromeritics
	SediGraph 5000D	
	BI-XDC	Brookhaven
Light obscuration	CIS-1	Galai
Electrical sensing zone	Multisizer II, Ta-II	Coulter
	MP-100	I.E.C.
	180XY	Elzone

Table 3
Number of models and data on the round robin

Principles	Aluminum oxide	Barium titanate	Boron nitride	Silicon nitride whisker
Electrical sensing zone	4	2	2	1
	15	9	10	10
Laser diffraction and scattering	8	8	8	8
	69	84	85	124
X-ray sedimentation	2	2		3
	12	12		17
Photosedimentation	5	6	6	2
	24	30	30	33
Light obscuration	1	1	1	1
	9	9	12	10

Upper: number of models; lower: number of data.

pattern of eddies in the suspension was clearly observed at the start of the measurements because of particle orientation, leading to the unstable measurement of initial transmitted light intensity. Ethylene glycol, having a higher viscosity, was therefore selected to minimize this particle orientation.

The dispersion effect of the suspension is influenced by the output power and type of the ultrasonic disrupter. Dispersion time was chosen as that time over which the size distribution became the same, regardless of the disrupters and output power used. Several types of ultrasonic baths (Sharp ut-604: output power 600 and 300 W, and Honda W103T:40 W) and one homogenizer (Nissei model us-300:300 W) were used. For the homogenizer, the ultrasonication time was determined to be 3 min for aluminum oxide, barium titanate and boron nitride, and 5 min for the silicon nitride whisker. For the baths, the ultrasonication time was determined to be 3 min for aluminum oxide and barium titanate, and 15 min for boron nitride and the silicon nitride whisker.

2.3.2. Measurement

The samples and instructions for the sample preparation conditions were distributed to the organizations who joined the round robin. All the measurements followed the same sample preparation conditions and procedure. The number of data obtained in the round robin is shown in Table 3.

3. Results

3.1. Particle size measured by various principles

Fig. 2 shows all the results of barium titanate measured by the laser diffraction and scattering method. The measured

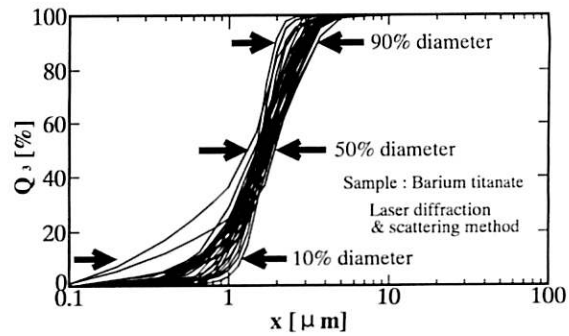

Fig. 2. Results of round robin for barium titanate measured by laser diffraction and scattering method. Eighty-four data measured by eight kinds of models are included in these results.

size distributions were represented by the average 10%, 50% and 90% diameters, and the data scattering was evaluated by the coefficient of variation of the represented diameters. These results are shown in Tables 4–6. The particle diameters measured by electrical sensing zone method are supposed to be the equivalent volume diameter which is not affected by particle shape [14]. Other principles were therefore discussed in comparison with the electrical sensing zone method, and the average measured diameter of each principle was divided by that of electrical sensing zone method. The ratios at the 10%, 50% and 90% diameters are defined as NR_{10}, NR_{50} and NR_{90}, respectively.

Figs. 3 and 4 show the results from the laser diffraction and scattering method and the X-ray sedimentation method, respectively. Fig. 5 shows the results of the photosedimentation method. Although the photosedimentation method belongs to the same measuring principle as X-ray sedimentation, the NR_{90} differs from that of X-ray sedimentation method in the case of rod-like particles. Fig. 6 shows the results from light obscuration. The NR_{50} is independent of the particle shape.

Table 4
Average 10% diameter and its coefficient of variation calculated from measured results of the round robin

Principles	Aluminum oxide	Barium titanate	Boron nitride	Silicon nitride whisker
Electrical sensing zone	1.16	0.94	3.65	1.24
	8.3	8.8	6.5	3.2
Laser diffraction and scattering	0.71	0.72	3.43	0.76
	35.9	30.7	18.5	22.3
X-ray sedimentation	0.95	1.03		0.85
	2.8	5.5		12.9
Photosedimentation	0.95	0.89	2.13	0.93
	14.2	17.5	29.4	14.0
Light obscuration	1.16	1.08	3.51	1.19
	6.0	2.3	9.1	5.2

Upper: average 10% diameter (μm), lower: variation coefficient (%).

Table 5
Average 50% diameter and its coefficient of variation calculated from measured results of the round robin

Principles	Aluminum oxide	Barium titanate	Boron nitride	Silicon nitride whisker
Electrical sensing zone	2.16	1.50	6.68	2.21
	9.8	2.3	5.6	3.6
Laser diffraction and scattering	2.10	1.66	8.79	3.11
	12.9	9.0	11.8	21.6
X-ray sedimentation	1.81	1.58		1.91
	3.0	2.9		7.3
Photosedimentation	1.69	1.44	4.96	2.32
	12.6	11.9	22.6	36.2
Light obscuration	2.88	1.80	7.41	2.29
	7.2	7.1	18.1	16.2

Upper: average 50% diameter (μm), lower: variation coefficient (%).

Table 6
Average 90% diameter and its coefficient of variation calculated from measured results of the round robin

Principles	Aluminum oxide	Barium titanate	Boron nitride	Silicon nitride whisker
Electrical sensing zone	4.07	2.16	11.04	4.70
	4.6	6.9	6.9	6.2
Laser diffraction and scattering	4.69	2.87	17.22	10.91
	9.6	15.3	17.3	27.5
X-ray sedimentation	3.68	2.46		4.75
	5.2	2.7		12.8
Photosedimentation	4.13	2.53	16.93	11.40
	41.8	14.7	51.4	98.2
Light obscuration	4.89	3.16	19.69	4.62
	3.2	6.1	35.2	7.6

Upper: average 90% diameter (μm), lower: variation coefficient (%).

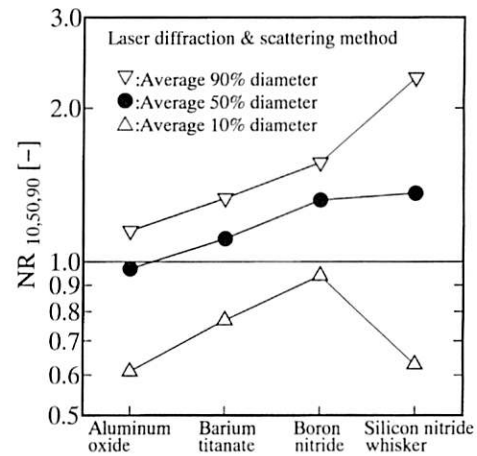

Fig. 3. Effect of particle shape on the particle size measured by the laser diffraction and scattering method.

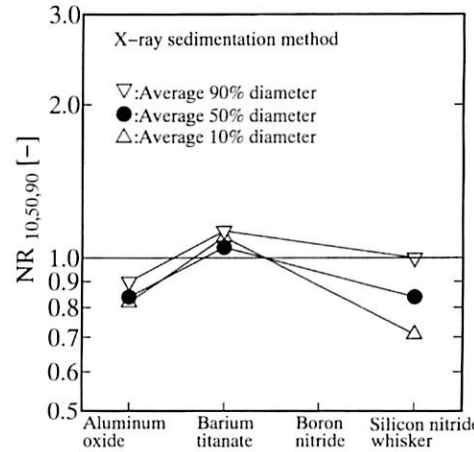

Fig. 4. Effect of particle shape on the particle size measured by the X-ray sedimentation method.

3.2. Range of the size distribution

The effect of particle shape on the range of size distribution was discussed using the following definition [2]:

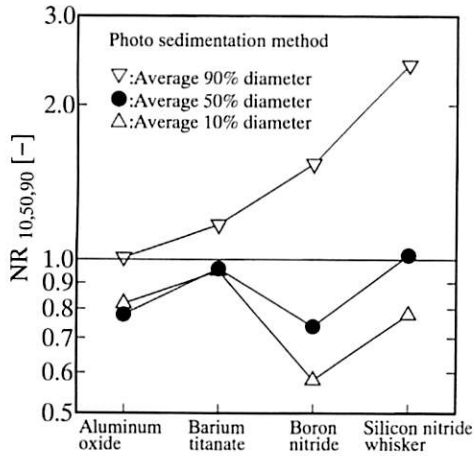

Fig. 5. Effect of particle shape on the particle size measured by the photosedimentation method.

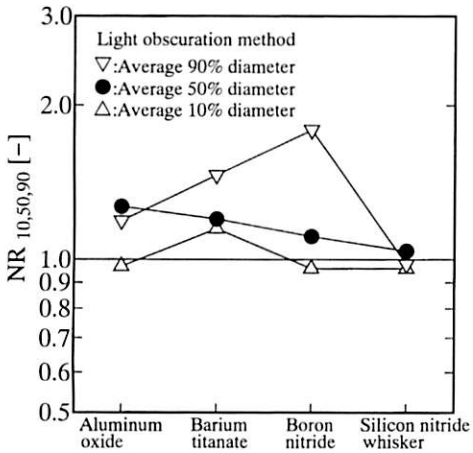

Fig. 6. Effect of particle shape on the particle size measured by the light obscuration method.

$$RD=(x_{90}-x_{10})/x_{50} \quad (1)$$

where x_{10}, x_{50} and x_{90} are the average diameters at 10%, 50% and 90%, respectively.

Fig. 7 shows the relationships between RD and powder samples. The RD value of the photosedimentation method is the largest and that of electrical sensing zone method is the smallest. In the measurement of anisotropic samples the RD changes with the measuring principles.

3.3. Scattering of the measured results

To discuss the effect of particle shape on the scatter of data measured with various equipment, the coefficients of variation at the average 10%, 50% and 90% diameters are summarized in Figs. 8–10, respectively. The coefficient of variation is approximately less than 30% of all average diameters. However, the data scatter is remarkably at the average 90% diameter of the anisotropic sample with the photosedimentation method.

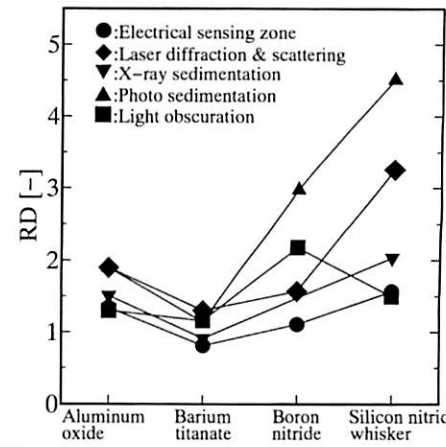

Fig. 7. Effect of particle shape on the range of size distribution (RD) measured by each method.

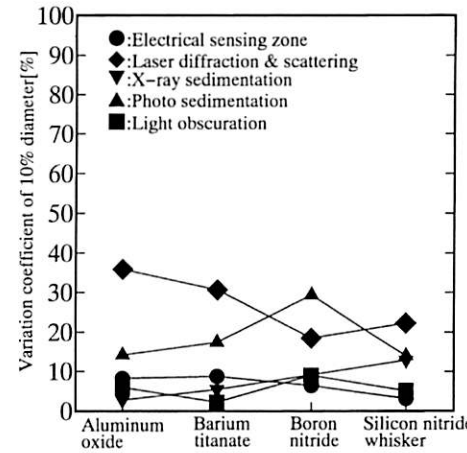

Fig. 8. Effect of particle shape on the data scattering of measured results at 10% diameter.

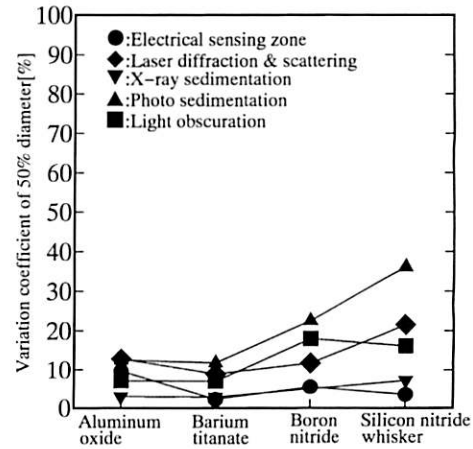

Fig. 9. Effect of particle shape on the data scattering of measured results at 50% diameter.

4. Discussion

4.1. Laser diffraction and scattering method

For anisotropic samples, the NR_{90} is much greater than that of isotropic samples, as shown in Fig. 3. In this method, the

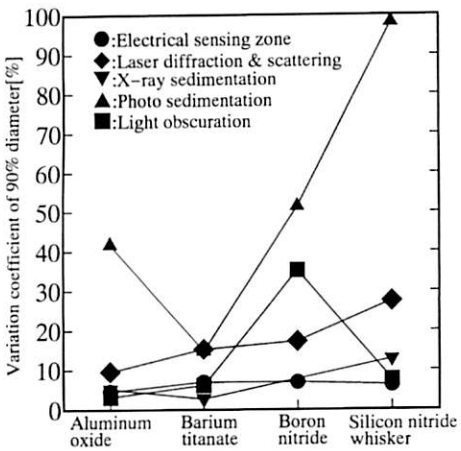

Fig. 10. Effect of particle shape on the data scattering of measured results at 90% diameter.

suspension flows through a narrow space (the clearance is approximately 2 mm) between two parallel glass cell walls. It is therefore supposed that the rod-like or flaky particles tend to orient along the direction of the flow. Since the laser beam is applied vertically to the glass cell, the light scattered by the oriented particles is measured. The scattered light pattern from the oriented rod-like particles is dissymmetrical and depends on the breadth and length of the particle [15,16]. It is probable that the average 90% and 10% diameters measured by this principle provide information on the length and breadth of the particles, and it can therefore be a reason why the NR_{90} and NR_{10} are far from 1 in Fig. 3. Since the average 10% diameter corresponds to the breadth and the average 90% diameter corresponds to the length, the range of size distribution is much wider than that measured by the electrical sensing zone method as shown in Figs. 3 and 7. Inaba and Matsumoto [2] reported that the range of size distribution of the rod-like particles measured by this principle is larger than that of electrical sensing zone method. These results suggest that since the range of the distribution is influenced by the particle elongation, this principle has a potential to evaluate the aspect ratio of rod-like particles.

Similar discussion is available for boron nitride. Since almost all flaky particles orient along the shear flow, they vertically face the applied laser beam in the flow cell and the size of the basal planes are mainly measured in this case. Therefore, the thickness of the particle can not be measured. This is the reason why the NR_{10} of boron nitride was not as small as that of the silicon nitride whisker.

4.2. X-ray sedimentation method

Regardless of the isotropic shape of aluminum oxide and barium titanate, the NR for each average diameter is smaller than 1 for aluminum oxide and larger than 1 for barium titanate, as shown in Fig. 4. As can be seen from the SEM photograph in Fig. 1a, the aluminum oxide contains the agglomerates. If these agglomerates cannot be broken down into the primary particles, the remaining agglomerates should settle more slowly than the rigid particles [4]. Therefore, since these agglomerates were apparently measured as small particles, the NR on aluminum oxide was smaller than 1. In contrast, the barium titanate contains few agglomerates as can be seen in Fig. 1b. The reason why the NR of barium titanate was larger than 1 is obviously due to the hydrodynamic effect related to its particle shape. The detail is discussed in Section 4.5, with the results for the silicon nitride whisker.

The scatter of the data measured by this principle is relatively small, as shown in Figs. 8–10, because of two possible reasons. One is that the transmittance intensity of X-rays is attenuated against the volume of the particle. This means that the transmitted intensity of the X-rays is independent of the particle shape and its orientation in the suspension. The other reason may be that only two or three models were compared as shown in Table 3.

4.3. Photosedimentation method

For the isotropic samples, the NR for each average diameter was almost always around 1 in as shown in Fig. 5. However, the NR_{90} was remarkably larger than 1 for the anisotropic samples. Furthermore, the data scatter for anisotropic samples was large in the coarse-size range as shown in Fig. 10.

As shown in Fig. 11, the results of the silicon nitride whisker are divided into two groups which are named group A and B. In the round robin, both the centrifugal sedimentation mode and the multimode were applied for the measurement. As in the multimode method, after gravitational sedimentation is completed for a given time, centrifugal sedimentation takes place. All the data measured in the centrifugal mode are included in group A, and the data measured in the multimode are almost all included in group B although a number of data are included in group A as well. Therefore, the difference in the measuring mode is the main reason why the data scattering for anisotropic sample is large as shown in Fig. 10.

In the multimode measurement, after a cuvette filled with suspension was shaken for mixing, it was placed in the equipment for measurement of gravitational sedimentation to start

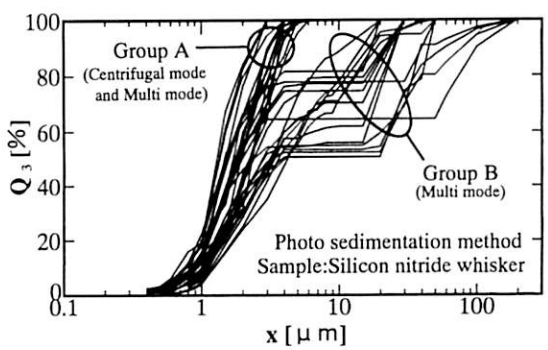

Fig. 11. Results of round robin for the silicon nitride whisker measured by photosedimentation.

at once. It is supposed that the liquid turbulence due to the shaking remains in the cuvette at the initial stage of the gravitational sedimentation. It was observed that the orientation of particles due to the anisotropy of the particle shape causes fluctuation in the initial detected transmittance intensity of light particularly for the flaky and rod-like particles and is the reason for the large scatter of the data from the multimode measurement, as shown in Fig. 11. The intensity fluctuation could be one reason for the NR_{90} of anisotropic sample being larger than 1, as shown in Fig. 5. However, it cannot be concluded from the data alone taken in this experiment. In the case of group B in Fig. 11, bimodal distributions were also observed. This result may be attributed to the configuration or the software of the equipment.

In the centrifugal mode of group A, the top size of the distribution was smaller than that measured in multimode. This is probably caused by the settling of the coarser particles under the centrifugal force.

4.4. Light obscuration method

In the measurement by light obscuration, the influence of particle shape was not clearly observed as shown in Fig. 6. In the light obscuration method, the agitated suspension in the cell is scanned by a rotating focused laser beam. The particle diameter is calculated from the interrupt period of the laser beam caused by the particle. In an agitated suspension, the anisotropic particles are considered to be randomly dispersed and it is therefore supposed that the results are less influenced by the particle shape.

4.5. Theoretical analysis for the sedimentation method

For the sedimentation method, the effect of various particle shapes on settling behavior under gravity can be explained by the dynamic shape factor [17]. When ellipsoidal particles settle in the purely viscous flow region, the dynamic shape factor is defined as the ratio of the resistance offered by dispersion media on the ellipsoidal particle to that on a spherical particle having the same volume. If the density of both particles is the same, the dynamic shape factor is expressed by the ratio of the square of the equivalent volume radius of a sphere (γ_e) to the sedimentation radius of ellipsoidal particle (γ_s) as follows [17].

$$\kappa=\gamma_e^2/\gamma_s^2 \qquad (2)$$

where κ is the dynamic shape factor.

The value of κ depends on the aspect ratio of the particle. Fig. 12 shows the relationships between the aspect ratio and the dynamic shape factor calculated by Fuchs [17]. The black circles show the settling of the particle in the direction of the major axis, and the white circles show the settling perpendicular to the major axis.

The silicon nitride whisker has an aspect ratio greater than 1, as shown in Fig. 1d. Furthermore, from the individual measurement of 400 particles observed under SEM, it was found that the average aspect ratio was 8. When this particle is assumed to be ellipsoidal with an aspect ratio of 8, κ can be read to be more than 1 from Fig. 12. In other words, this means that the sedimentation radius of this silicon nitride whisker particle is smaller than its equivalent volume radius of the sphere. In practice, as shown in Fig. 4, the NR of silicon nitride whisker is obviously smaller than 1.

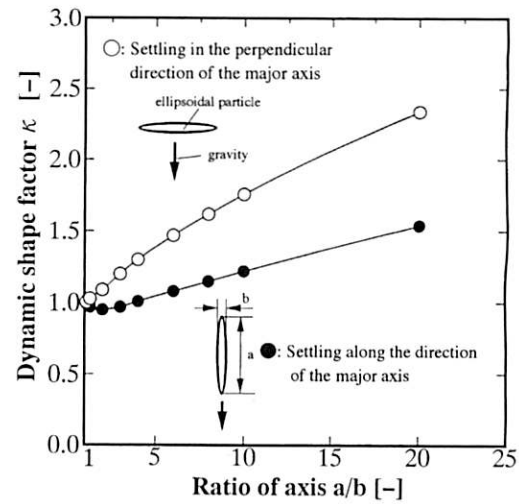

Fig. 12. Relationship between dynamic shape factor and the aspect ratio of ellipsoidal particles.

The barium titanate shown in Fig. 1b seems to be ellipsoidal with an aspect ratio of around 1.5. Therefore, κ less than 1 can be taken from Fig. 12 depending on the particle orientation. In this case, the sedimentation radius of these particles is larger than their equivalent volume radius of the sphere. This may be a reason why the NR of barium titanate was larger than 1 as shown in Fig. 4.

These results on the silicon nitride whisker and barium titanate support the idea that the results obtained by X-ray sedimentation can be explained theoretically based on the dynamic shape factor. Also for the photosedimentation method, although it belongs to the same measuring principle as X-ray sedimentation, the NR_{90} did not agree with that of the X-ray sedimentation method as shown in Fig. 5. One reason may be that the particle settling in the static fluid was hindered by the convection flow generated in the suspension at the initial stage of measurement as described before.

4.6. The relationships between RD and NR_{90}

The relationships between RD and NR_{90} for barium titanate, boron nitride and the silicon nitride whisker are shown in Figs. 13–15. The value of RD and NR_{90} of barium titanate are around 1 as shown in Fig. 13. For boron nitride the RD increases with the NR_{90} as shown in Fig. 14 and a similar tendency is also observed for the result of the silicon nitride whisker as shown in Fig. 15. These results indicate that RD is significantly influenced by the NR_{90} for the measurement of anisotropic samples.

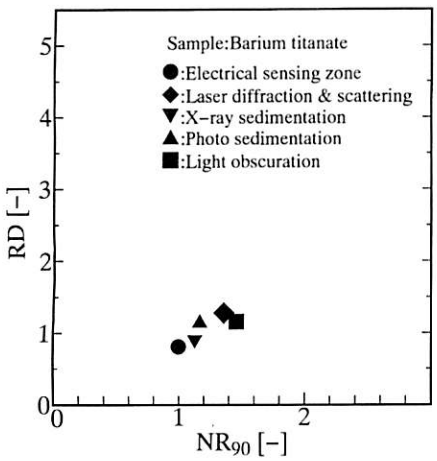

Fig. 13. Relationship between RD and NR_{90} for barium titanate.

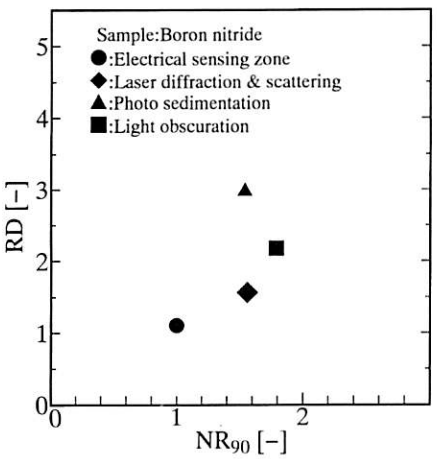

Fig. 14. Relationship between RD and NR_{90} for boron nitride.

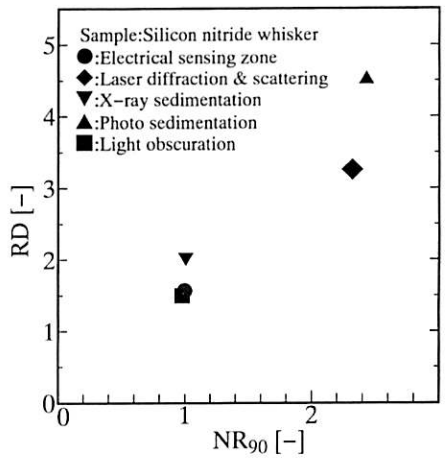

Fig. 15. Relationship between RD and NR_{90} for the silicon nitride whisker.

5. Conclusions

The effect of particle shape on particle size measured by various principles is discussed. Furthermore, the dependence of the particle shape on the range of the distribution and the scattering of the measured results was analyzed on the basis of the round robin results. The following conclusions were obtained.

(1) In the measurement of anisotropic particles such as flaky and rod-like particles, the effect of particle shape on the particle size is much larger than that for block-shaped particles.

(2) In the laser diffraction and scattering method and the photosedimentation method, the size range and scattering of the measured distributions change drastically with the particle shape compared to those obtained by X-ray sedimentation and light obscuration methods.

(3) For the measurement of anisotropic samples by laser diffraction and scattering method, the range of size distribution is large because of particle orientation along the shear flow. Particularly, for the measurement of rod-like particles, this principle has the potential to evaluate the aspect ratio.

(4) In the X-ray sedimentation method, the effect of particle shape on the measured results is small. Because the transmittance intensity of X-rays is independent of the particle shape and its orientation, the equivalent volume diameter can be measured. The effect of the particle shape on the measured particle size can be explained by the theoretical analysis based on the dynamic shape factor.

(5) In the photosedimentation method, the effect of particle shape on the measured results is remarkably large in the coarse-size range of the distribution. It is because the particle orientation due to the turbulence of the liquid produces an intensity fluctuation of the transmitted light at the initial stage of the gravitational sedimentation.

(6) The effect of particle shape is not clearly observed in the measurement by light obscuration method because the anisotropic particles are dispersed at random in the agitated suspension.

6. Nomenclature

NR	normalized ratio with electrical sensing zone method (−)
Q_3	cumulative mass % (%)
RD	range of particle size distribution (−)
x	particle diameter (μm)

Greek letters

γ_e	equivalent volume radius of sphere (μm)
γ_s	sedimentation radius of ellipsoid (μm)
κ	dynamic shape factor (−)

Subscripts

10, 50, 90	cumulative mass at 10%, 50% and 90%

Acknowledgements

The authors gratefully acknowledge all participants who joined the round robin for their great cooperation and also wish to thank the members of the advisory committee of this project for their beneficial support.

References

[1] M. Arakawa, T. Yokoyama, T. Yamaguchi, T. Minami, J. Soc. Mater. Sci. Jpn. 32 (1983) 966.
[2] K. Inaba, K. Matsumoto, J. Soc. Powder Technol., Jpn. 32 (1995) 722.
[3] O. Hayakawa, K. Nakahira, J. Tsubaki, J. Ceram. Soc. Jpn. 103 (1995) 392.
[4] O. Hayakawa, K. Nakahira, J. Tsubaki, J. Ceram. Soc. Jpn. 103 (1995) 500.
[5] O. Hayakawa, K. Nakahira, J. Tsubaki, J. Ceram. Soc. Jpn. 103 (1995) 586.
[6] S.H. Kang, P.J. Rhew, D.W. Kim, J.H. Park, in: Soc. Powder Technol., Jpn. (Ed.), Proc. Second World Congress Particle Technology, Kyoto, Japan, 1991, p. 386.
[7] C.M.G. Heffels, D. Heitzmann, E.D. Hirleman, H.J.M. Kramer, B. Scarlett, in: Proc. the Third International Congress on Optical Particle Sizing, Yokohama, Japan, 1993, p. 23.
[8] K. Muinonen, K. Lumme, J. Peltoniemi, W.M. Irvine, Appl. Opt. 28 (1989) 3051.
[9] C. Bernhardt, in: N. Stanley-Wood, R. Lines (Eds.), Proc. the 25th Anniversary Conf. Particle Size Analysis '91, Loughborough, 1991.
[10] R.C. Weast, M.J. Astel, W.H. Beyer (Eds.), Handbook of Chemistry and Physics, 68th edn., CRC Press, Boca Raton, FL, 1987.
[11] Ge ve Samusonofu, Hikinzoku Chikkabutsu, Nisso tsuushin-sha, Japan, 1971.
[12] Malvern instrument, Index of the Assistance of Master Sizer Users, UK, 1990.
[13] O. Hayakawa, J. Tsubaki, J. Soc. Powder Technol., Jpn. 30 (1993) 324.
[14] T. Allen, Particle Size Measurement, 4th edn., Chapman and Hall, London, 1990.
[15] E.F. Aharonson, N. Karasikov, M. Roitberg, J. Shamir, J. Aerosol Sci. 17 (1986) 530.
[16] C.F. Bohren, D.R. Huffman, Absorption and Scattering of Light by Small Particles, Wiley, New York, 1983.
[17] N.A. Fuchs, The Mechanics of Aerosols, Pergamon Press, Oxford, 1964.